scientific reports

Check for updates

OPEN

Impaired mitochondrial medium-chain fatty acid oxidation drives periportal macrovesicular steatosis in sirtuin-5 knockout mice

Eric S. Goetzman[1,5]✉, Sivakama S. Bharathi[1], Yuxun Zhang[1], Xue-Jun Zhao[1], Steven F. Dobrowolski[2], Kevin Peasley[1], Sunder Sims-Lucas[1] & Satdarshan P. Monga[3,4,5]

Medium-chain triglycerides (MCT), containing C_8–C_{12} fatty acids, are used to treat several pediatric disorders and are widely consumed as a nutritional supplement. Here, we investigated the role of the sirtuin deacylase Sirt5 in MCT metabolism by feeding Sirt5 knockout mice (Sirt5KO) high-fat diets containing either C_8/C_{10} fatty acids or coconut oil, which is rich in C_{12}, for five weeks. Coconut oil, but not C_8/C_{10} feeding, induced periportal macrovesicular steatosis in Sirt5KO mice. ^{14}C–C_{12} degradation was significantly reduced in Sirt5KO liver. This decrease was localized to the mitochondrial β-oxidation pathway, as Sirt5KO mice exhibited no change in peroxisomal C_{12} β-oxidation. Endoplasmic reticulum ω-oxidation, a minor fatty acid degradation pathway known to be stimulated by C_{12} accumulation, was increased in Sirt5KO liver. Mice lacking another mitochondrial C_{12} oxidation enzyme, long-chain acyl-CoA dehydrogenase (LCAD), also developed periportal macrovesicular steatosis when fed coconut oil, confirming that defective mitochondrial C_{12} oxidation is sufficient to induce the steatosis phenotype. Sirt5KO liver exhibited normal LCAD activity but reduced mitochondrial acyl-CoA synthetase activity with C_{12}. These studies reveal a role for Sirt5 in regulating the hepatic response to MCT and may shed light into the pathogenesis of periportal steatosis, a hallmark of human pediatric non-alcoholic fatty liver disease.

The sirtuin deacylase Sirt5 is one of seven mammalian sirtuins that remove lysine acylation post-translational modifications (PTMs) from cellular proteins. Sirt5 is unique in the sirtuin family for its specificity in removing succinyl, glutaryl, and malonyl groups from lysine residues[1–3]. While its main site of action is the mitochondria, Sirt5 is also the only sirtuin shown to localize to peroxisomes[4]. In liver mitochondria, Sirt5 desuccinylation positively regulates fatty acid oxidation (FAO) and ketogenesis, the process by which FAO-derived acetyl-CoA is converted to ketone bodies for secretion to the periphery[3,5]. Interestingly, in the peroxisome, which possesses a parallel FAO pathway to that found in mitochondria, Sirt5 negatively regulates the key FAO protein acyl-CoA oxidase-1 (ACOX1)[4]. Based on these studies, it would be predicted that deleting Sirt5 would suppress mitochondrial FAO while promoting peroxisomal FAO. However, this has not been directly tested. Here, we investigated the effect of Sirt5 deletion on FAO in mice maintained on a high-fat coconut oil diet. Unlike the lard-based high-fat diets typically used in rodent studies, coconut oil has very little long-chain fatty acids. Rather, coconut oil is rich in medium-chain triglycerides (MCT).

MCT, defined as triglycerides containing fatty acids C_8 to C_{12} in length, have a broad significance to human health. MCT are a key component of nutritional formulas given to premature infants[6]. MCT are also used to treat long-chain fatty acid oxidation disorders, gastrointestinal disorders, and epilepsy, among others[7–9]. Recently, consumption of MCT as a nutritional supplement has increased tremendously due to the popularity of ketogenic diets for weight loss[10]. Medium-chain fatty acids released from MCT in the gut are poor substrates for re-synthesis of triglycerides within enterocytes, and as a result they are absorbed into the portal vein as free acids and send to

[1]Department of Pediatrics, Children's Hospital of Pittsburgh of UPMC, University of Pittsburgh School of Medicine, Pittsburgh, PA, USA. [2]Department of Pathology, University of Pittsburgh School of Medicine, Pittsburgh, PA, USA. [3]Division of Experimental Pathology, Department of Pathology, University of Pittsburgh School of Medicine, Pittsburgh, PA, USA. [4]Division of Gastroenterology, Hepatology and Nutrition, Department of Medicine, University of Pittsburgh School of Medicine, Pittsburgh, PA, USA. [5]Pittsburgh Liver Research Center, University of Pittsburgh Medical Center, University of Pittsburgh School of Medicine, Pittsburgh, PA, USA. ✉email: eric.goetzman@chp.edu

the liver for disposal. Less than 1% of the ingested dose of MCT will reach peripheral circulation[11]. Consumption of large doses of MCT exposes hepatocytes to high concentrations of free medium-chain fatty acids, which must be either immediately catabolized or else elongated to a chain length that can be stored as triglyceride. This contrasts with long-chain fatty acids released from long-chain triglycerides (LCT), which are re-esterified into triglycerides, packed into chylomicrons, and trafficked from the gut through the lymphatic system and into peripheral circulation.

Not all MCT-based nutritional products contain the same composition of fatty acids. Coconut oil is primarily C_{12} (50%), but also contains minor amounts of C_{14}, C_{10}, and C_8[12]. Other MCT products contain either pure C_8 or a mixture of C_8 and C_{10} obtained from fractionating coconut oil. C_8/C_{10} may undergo a different route of metabolism than C_{12} due to the substrate specificity and intracellular localization of the acyl-CoA synthetase enzymes responsible for conjugating free fatty acids to acyl-CoAs, which are the biologically active form of fatty acids in the cell. C_8, and to lesser extent C_{10}, can diffuse into the mitochondrial matrix where they are activated into acyl-CoAs by the medium-chain acyl-CoA synthetases (ACSMs)[13]. C_{12} cannot cross the mitochondrial membrane and is a poor substrate for ACSMs[13]. C_{12} is activated to C_{12}-CoA by the long-chain acyl-CoA synthetases (ACSLs), which reside on the outer mitochondrial membrane, plasma membrane, ER, and the peroxisomal membrane[14]. In keeping with this, C_{12} can be catabolized by both mitochondrial and peroxisomal β-oxidation pathways[15]. C_{12} is also metabolized by a minor pathway known as ω-oxidation in which C_{12} is hydroxylated by cytochrome P450 enzymes in the endoplasmic reticulum, converted to a dicarboxylic acid in the cytosol, and finally chain-shortened in the peroxisome[16]. While peroxisomes can chain-shorten long-chain fatty acids down to C_6[17] and DCAs as far as C_4[18], the capacity of the peroxisome to catabolize exogenous C_8/C_{10} is limited by the fact that all known ACSMs reside in the mitochondrial matrix[19].

In rodent models, both C_8 and C_{12} feeding have been linked to hepatic steatosis[15,20]. However, other studies have indicated either no fat accumulation or even a reversal of pre-existing fatty liver, leading to the suggestion that MCT may have utility for treating the metabolic syndrome[21,22]. Understanding the molecular mechanisms involved in hepatic adaptation to MCT is critical for determining the impact of this supplement on human health. Because of Sirt5's dual localization to mitochondria and peroxisomes and its known opposite regulation of FAO enzymes in these compartments, we used Sirt5 knockout mice to interrogate the role of this lysine deacylase on the hepatic response to dietary C_8/C_{10} versus coconut oil. Our results implicate Sirt5 as an important regulator of C_{12} disposal in the liver.

Results

Sirt5KO mice develop hepatic macrovesicular steatosis on coconut oil diet. To study the role of Sirt5 in regulating the hepatic response to acute high-fat feeding, we placed Sirt5KO and wild-type control mice on three high-fat diets containing different chain-lengths of fatty acids: (1) a diet containing 60% C_8 and 40% C_{10}; (2) a coconut-oil diet containing primarily C_{12}; and (3) a long-chain triglyceride (LCT) diet containing primarily C_{16} and C_{18} fatty acids. The relative composition of these diets appears in Supplemental Fig. 1. A low-fat standard diet (SD) served as control. After five weeks on the high-fat diets, liver tissue was collected and analyzed for signs of steatosis. In H&E-stained liver sections, macrovesicular steatosis was noted only in Sirt5KO livers from mice maintained on the coconut oil diet (Fig. 1a,b). This was observed in both genders of Sirt5KO mice. While the C_8/C_{10} diet did not induce overt macrovesicular steatosis, increased microvesicular lipid deposition was visible in liver of both genotypes upon Oil-Red-O staining (Fig. 2). The intensity of the Oil-Red-O staining was even greater with coconut oil feeding. Little or no Oil-Red-O staining was visible in livers from mice fed LCT for five weeks. Together, the H&E and Oil-Red-O stains indicated that fat accumulated in the order of coconut > > C_8/C_{10} > > LCT for both genotypes of mice, with the lipid accumulation progressing to the point of macrovesicular steatosis only in Sirt5KO mice on coconut oil diet. This was supported by a biochemical analysis of liver triglyceride content. Both C_8/C_{10} and coconut oil feeding significantly increased the triglyceride content of liver tissue over that seen in liver from mice maintained on the SD, while LCT had no effect (Fig. 1c). Sirt5 deficiency was associated with significantly increased liver triglycerides for both the C_8/C_{10} and coconut oil diets (Fig. 1c). Again, both genders were evaluated, and no gender effect was seen for triglyceride accumulation.

The macrovesicular steatosis in coconut oil-fed Sirt5KO mice is periportal. In adult humans with non-alcoholic fatty liver disease (NAFLD) and NAFLD rodent models induced by chronic LCT feeding, macrovesicular steatosis first appears around the pericentral regions of the liver. In contrast, pediatric NAFLD is characterized by periportal steatosis[23]. Interestingly, while five weeks of coconut oil feeding induced pan-zonal microvesicular steatosis in both wild-type and Sirt5KO livers as visualized by Oil-Red-O staining (Fig. 2), the macrovesicular steatosis in Sirt5KO livers was strictly periportal (Fig. 3a,b). To confirm the periportal localization of the lipid droplets we immunostained the liver tissue for glutamine synthase (GS), a marker of the pericentral zone. No lipid droplets were observed near the GS-positive pericentral zones (Fig. 3c–f). Besides marking the pericentral zones, the GS immunostaining highlighted an altered morphology of the pericentral hepatocytes in Sirt5KO liver that was consistent with ballooning degeneration. Sirt5 has previously been reported to exhibit hepatic zonation, with higher expression in primary mouse hepatocytes isolated from the periportal zone[24]. We confirmed this using beta-galactosidase staining as a proxy for expression of the Sirt5 mutant allele in Sirt5KO mice, which contains a lacZ insert. Pericentral hepatocytes exhibited less staining for the Sirt5 promoter-driven beta-galactosidase enzyme (Fig. 3g).

Sirt5KO liver has decreased capacity for C_{12} fatty acid β-oxidation (FAO). We next sought to investigate the mechanism(s) behind the observed acceleration in lipid storage in Sirt5KO livers during coconut oil feeding. Sirt5KO mice have previously been shown to be deficient in long-chain FAO but have not been

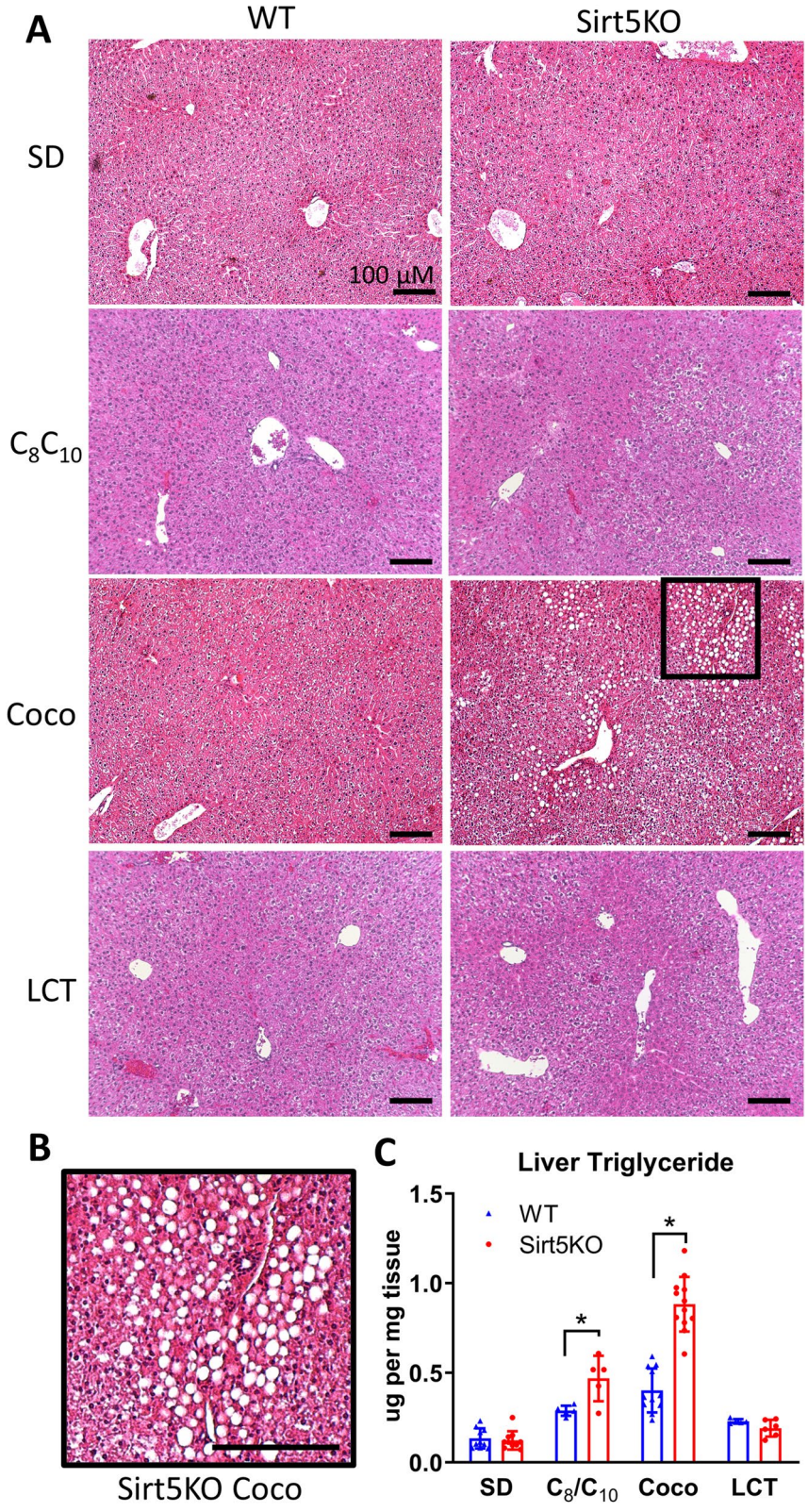

Figure 1. Sirt5KO mice develop hepatic macrovesicular steatosis on coconut oil diet. **(A)** Representative hematoxylin and eosin liver tissue staining from wild-type and Sirt5KO mice maintained on four different diets for five weeks: standard diet (SD), high-fat C_8/C_{10} diet, high-fat coconut oil diet (Coco), or high-fat long-chain triglyceride (LCT) diet. The relative composition of these diets is illustrated in Supplemental Fig. 1. Fat droplets were visible in only coconut-fed Sirt5KO mice. Scale bar, 100 µM. **(B)** Inset from coconut-fed Sirt5KO liver in panel **(A)**, showing lipid droplets at a higher resolution. **(C)** Liver triglyceride content of mice maintained on the four diets for five weeks. N = 6 for C_8/C_{10} and LCT diets, and N = 10 for coconut and SD diets. There was no gender difference in triglyceride accumulation; all groups contained half males and half females, age 6–8 weeks at time of diet onset. *P < 0.01 Sirt5KO versus wild-type controls.

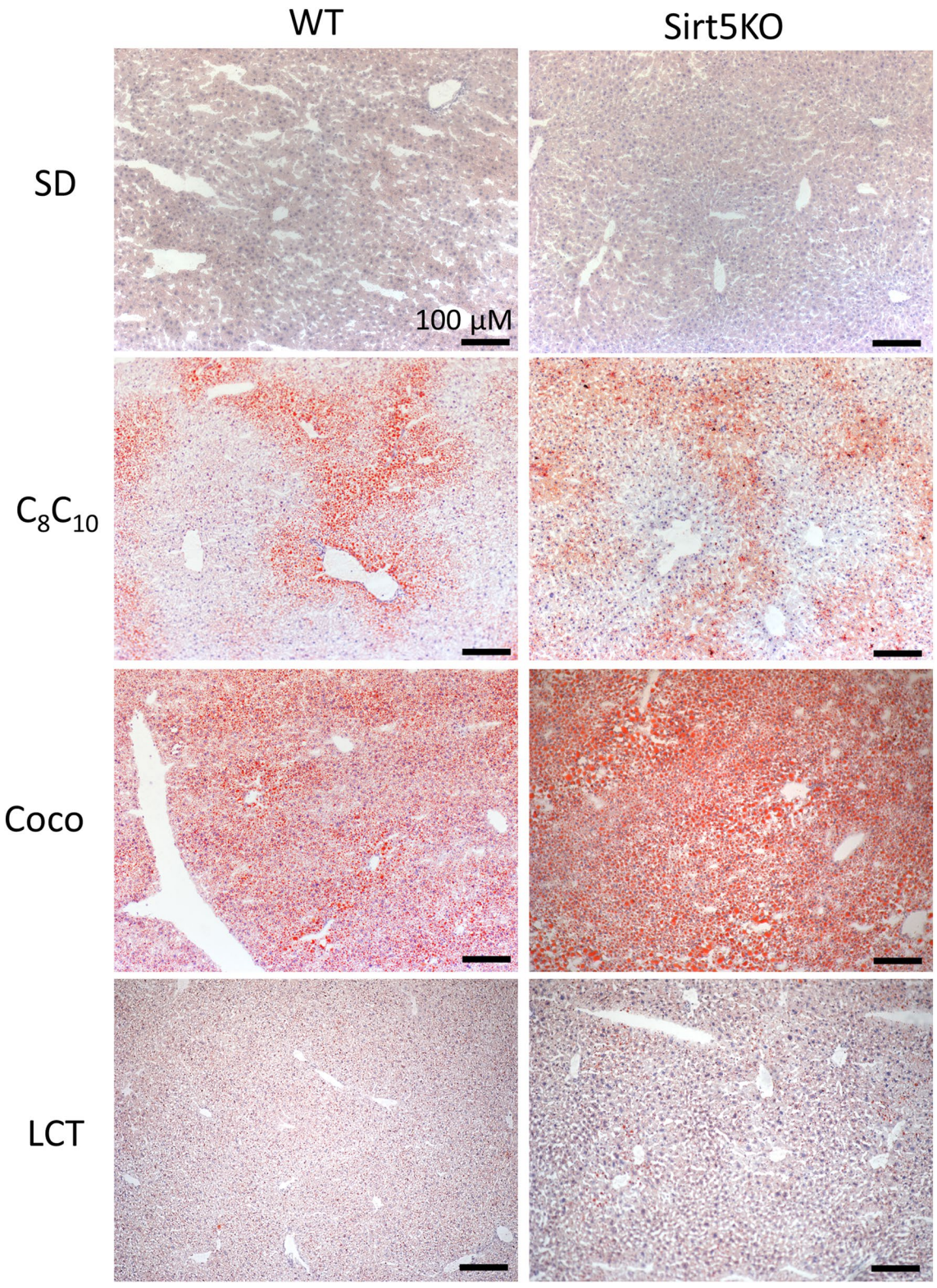

Figure 2. Oil-Red-O staining reveals steatosis in both C_8/C_{10} and coconut-fed mice. Representative Oil-Red-O stained liver tissue from wild-type (WT) and Sirt5KO mice on four different diets: standard diet (SD), C_8/C_{10} diet, coconut oil diet (Coco), and long-chain triglyceride diet (LCT). Scale bar, 100 µM.

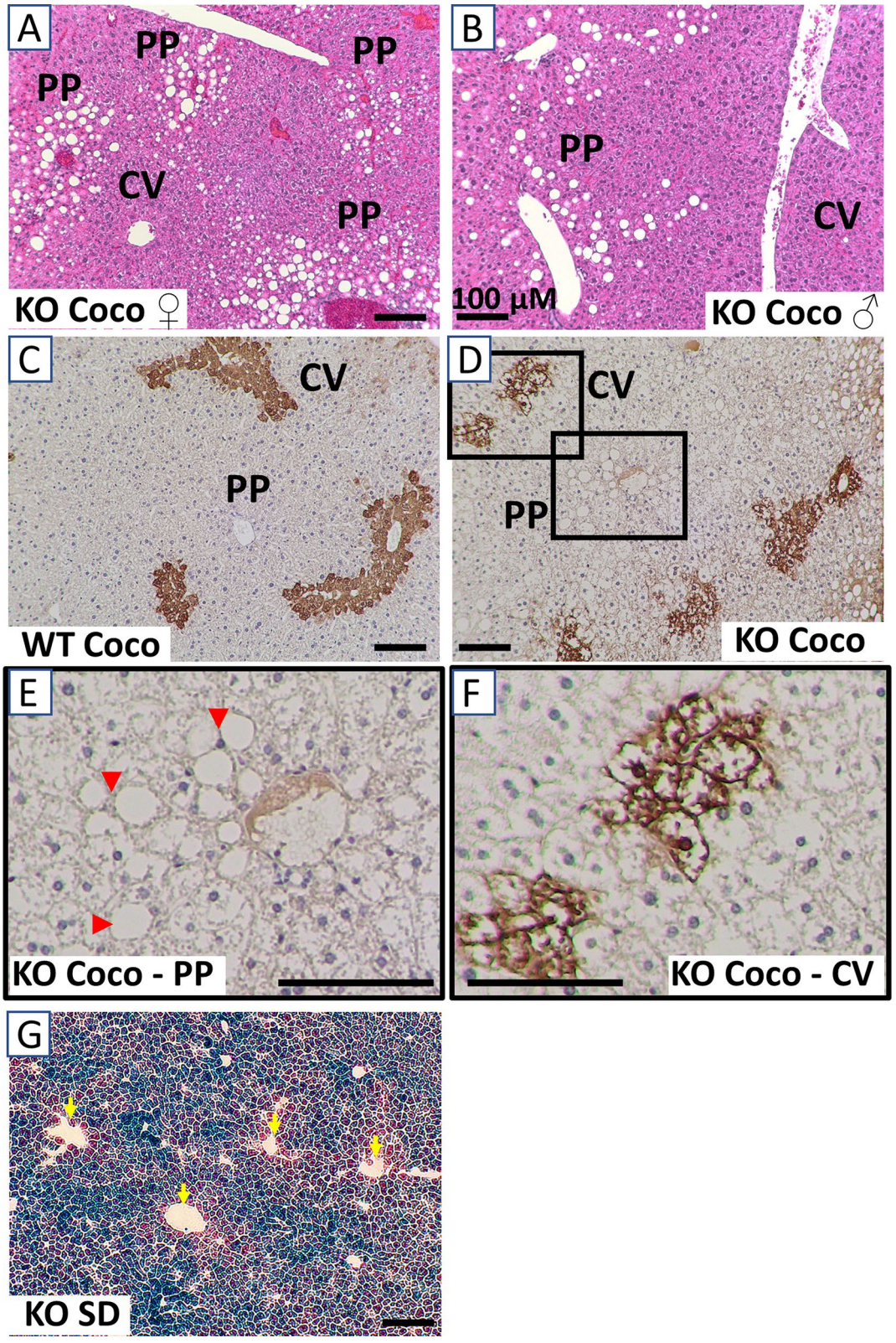

Figure 3. The macrovesicular steatosis in coconut oil-fed Sirt5KO mice is periportal. Both female **(A)** and male **(B)** coconut-fed Sirt5KO mice showed formation of lipid droplets in the periportal (PP) regions but not central vein (CV) regions as gauged by a pathologist's examination of hematoxylin/eosin-stained liver. **(C)** Liver tissue from coconut-fed wild-type and **(D)** Sirt5KO mice, immunostained for glutamine synthase (GS), a marker of pericentral hepatocytes. **(E,F)** Close-up images of inset areas from **(D)**, showing a periportal region **(E)** and a pericentral region **(F)** from a coconut-fed Sirt5KO liver. Periportal lipid droplets are indicated with arrow heads in **(E)**; no droplets are visible in **(F)**. Note the ballooning degeneration in **(F)**. **(G)** β-galactosidase staining for Sirt5 expression in Sirt5KO liver. The mutant allele in Sirt5KO mice contains a lacZ insert, and β-gal staining can be used as a proxy for Sirt5 expression. Blue staining is less intense around the central veins, indicated with yellow arrowheads. Scale bar, 100 µM.

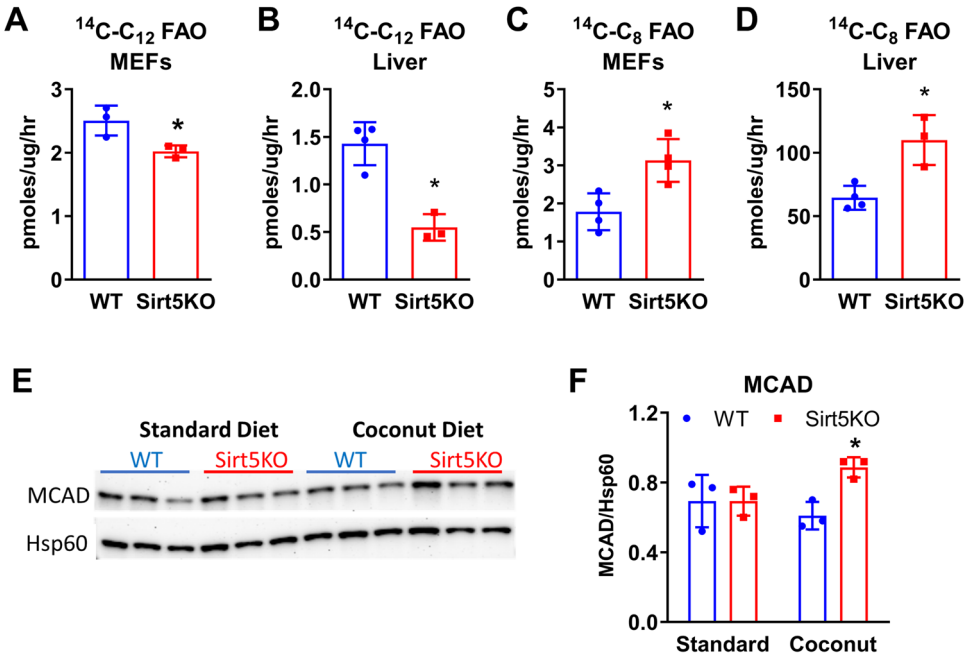

Figure 4. Sirt5KO liver has decreased capacity for C_{12} fatty acid oxidation. **(A)** ^{14}C–C_{12} flux to labeled acid-soluble metabolites in wild-type and Sirt5KO mouse embryonic fibroblasts (MEFs); **(B)** ^{14}C–C_{12} FAO flux in coconut-fed liver homogenates. **(C)** ^{14}C–C_8 flux to acid-soluble metabolites in MEFs and **(D)** coconut-fed liver homogenates. **(A–D)** are data from N = 3–4 biological replicates. **(E)** Immunoblotting for MCAD in liver from SD and coconut-fed WT and Sirt5KO mice, with heat-shock protein-60 (Hsp60) as a mitochondrial loading control. The uncropped version of these blots appears in Supplemental Fig. 2. **(F)** Densitometric analysis of blot in panel **(E)**, MCAD/Hsp60. *P < 0.05 for Sirt5KO versus wild-type control.

evaluated for changes in medium-chain FAO[3]. To interrogate medium-chain FAO we used ^{14}C-labeled C_8 and C_{12} and quantified flux in liver homogenates as well as mouse embryonic fibroblasts (MEFs). Sirt5KO MEFs, cultured in standard medium, showed a significant deficit in ^{14}C-C_{12} catabolism (Fig. 4a). In contrast, C_8 oxidation rates were higher in Sirt5KO MEFs (Fig. 4c). The same pattern was observed in liver homogenates prepared from mice fed coconut oil diet for five weeks (Fig. 4b,d). The higher C_8 oxidation may be due to higher expression of the C_8-specific enzyme medium-chain acyl-CoA dehydrogenase (MCAD) in Sirt5KO livers after coconut oil feeding (Fig. 4e,f).

Peroxisomal FAO is not altered in coconut-fed Sirt5KO mice. C_{12}, the principal fatty acid in coconut oil, is the optimal substrate for the rate-limiting peroxisomal FAO enzyme acyl-CoA oxidase-1 (ACOX1)[25]. In wild-type mouse liver homogenates from animals on standard diet, nearly 40% of the capacity for ^{14}C–C_{12} oxidation was resistant to potassium cyanide (KCN) and therefore peroxisomal (Fig. 5a). In contrast, for the long-chain fatty acid (C_{16}), peroxisomes contributed only about 10% (Fig. 5b). Because of the strict mitochondrial localization of the acyl-CoA synthetases responsible for activation of C_8 to C_8-CoA, C_8 metabolism is believed to be mitochondria-specific[19]. We therefore reasoned that the low C_{12} oxidation in Sirt5KO liver, but normal/high C_8 oxidation (Fig. 4), might be due to a specific loss of peroxisomal FAO capacity. Western blotting indicated a significant increase in ACOX1 protein expression in both genotypes of mice when fed coconut oil diet for five weeks (Fig. 5c,d). Immunostaining for the peroxisomal marker protein PMP70 showed that peroxisomes are more enriched in the pericentral zones when mice are maintained on a standard diet but demonstrate a pan-zonal proliferation after five weeks of coconut oil diet (Fig. 5e). This occurred in both wild-type and Sirt5KO mice, but overall, the PMP70 staining was darker in Sirt5KO liver. However, the rate of KCN-resistant (peroxisomal) ^{14}C–C_{12} FAO in liver homogenates of coconut oil-fed mice was not significantly different between genotypes (Fig. 5f). This indicates that the reduced capacity for C_{12} oxidation seen in Sirt5KO liver is not attributable to suppressed peroxisomal FAO.

Fatty acid ω-oxidation is upregulated in Sirt5KO livers. In addition to mitochondria and peroxisomes, C_{12} is also the optimal chain length for a minor FAO pathway known as ω-oxidation[16]. ω-oxidation initiates with C_{12} hydroxylation by Cyp4a family members in the ER. Through a poorly characterized pathway, $C_{12}OH$ is converted to a dicarboxylic C_{12} fatty acid (DC_{12}) and finally catabolized by peroxisomes, with only minimal contribution by mitochondria[26]. Immunoblotting revealed significantly higher protein expression of enoyl-CoA hydratase/3-hydroxy-CoA dehydrogenase (EHHADH), a peroxisomal enzyme known to be required for DC_{12} catabolism[27], in Sirt5KO liver following five weeks on coconut oil diet (Fig. 6a,b). DC_{12} is chain-shortened to adipic acid which is excreted into the urine. Sirt5KO mice on coconut-oil diet excreted

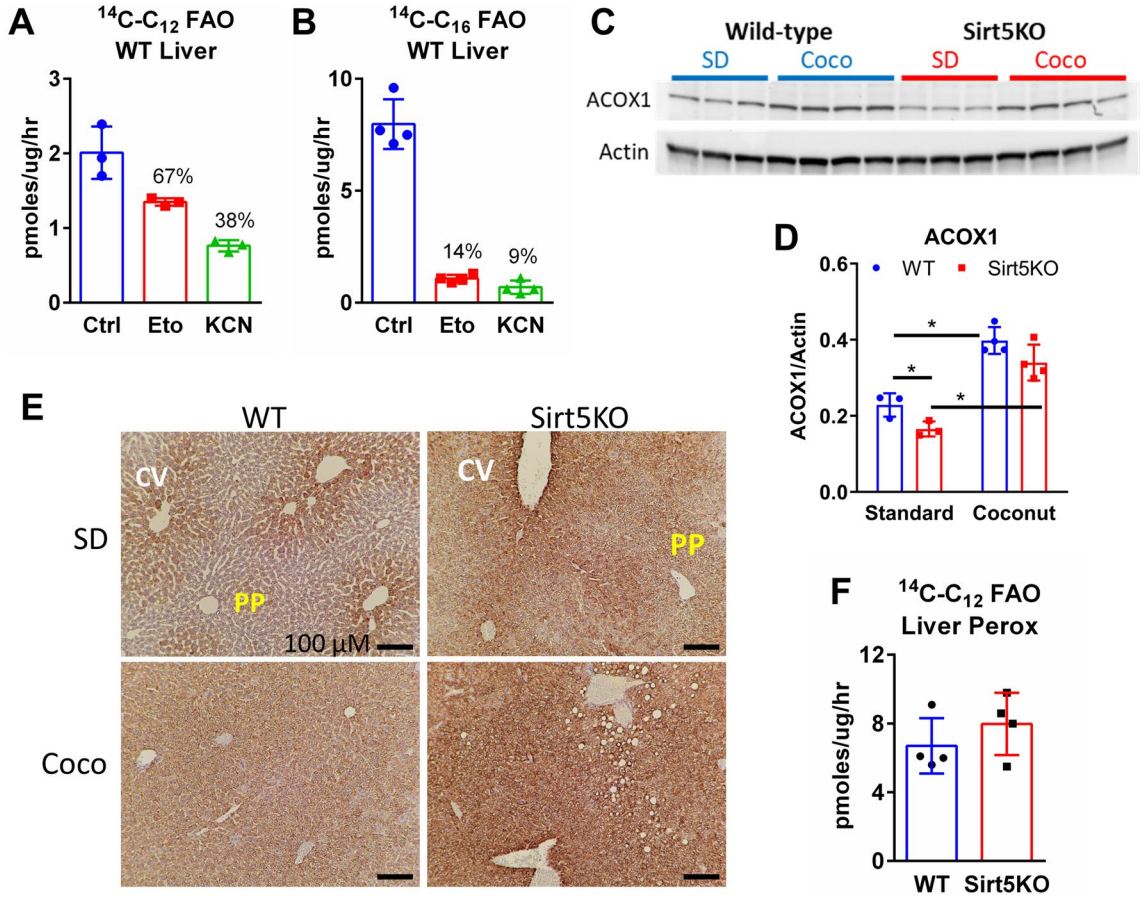

Figure 5. Peroxisomal FAO is not altered in Sirt5KO mice on coconut oil diet. **(A)** Effect of mitochondrial FAO inhibitors on $^{14}C–C_{12}$ and **(B)** $^{14}C–C_{16}$ flux to acid-soluble metabolites. Flux to acid-soluble metabolites was assayed in the presence of either 100 µM of the irreversible Cpt1 inhibitor etomoxir or 2 mM of the respiratory chain inhibitor KCN. **(C)** Immunoblotting for peroxisomal acyl-CoA oxidase-1 (ACOX1) in standard diet (SD, N = 3) and coconut-fed (Coco, N = 4) wild-type and Sirt5KO livers, with β-actin as loading control. The uncropped versions of these blots appear in Supplemental Fig. 3. **(D)** Densitometric analysis of immunoblot in panel C, expressed as ACOX1/β-actin. *P < 0.01 for indicated pairwise comparisons. **(E)** Representative immunostaining of liver tissue from standard diet and coconut-fed with anti-PMP70 antibody, a peroxisomal membrane protein. Note the darker staining around the central vein (CV) compared to periportal (PP) tracts on standard diet. Scale bar, 100 µM. **(F)** $^{14}C–C_{12}$ peroxisomal fatty acid oxidation, measured as KCN-resistant flux to labeled acid-soluble metabolites, N = 4 liver homogenates from coconut-fed mice.

four-fold more adipic acid than wild-type (Fig. 6c). Finally, higher ^{14}C-DC$_{12}$ oxidation was observed in Sirt5KO MEFs (Fig. 6d). An attempt was made to measure ^{14}C-DC$_{12}$ oxidation in liver, but the substrate was found to be unsuitable for assaying broken cells or tissue homogenates. Together these data suggest increased utilization of the ω-oxidation pathway in the absence of Sirt5.

Loss of mitochondrial C_{12} FAO causes periportal macrovesicular steatosis on coconut oil-diet. The observations of normal peroxisomal C_{12} oxidation and elevated ω- oxidation in Sirt5KO mice suggested that the defect in C_{12} metabolism must be mitochondrial. The first step in mitochondrial FAO is catalyzed by the acyl-CoA dehydrogenase (ACAD) enzyme family. There are four ACAD enzymes with partially overlapping substrate specificities[28]. To determine which ACADs contribute to C_{12}-CoA metabolism, we compared the specific activities of all four recombinant enzymes with C_{12}-CoA. Long-chain acyl-CoA dehydrogenase (LCAD) exhibited the highest specific activity with C_{12}-CoA, followed by MCAD (Fig. 7a). Very long-chain acyl-CoA dehydrogenase (VLCAD) had low activity with C_{12}-CoA and ACAD9 activity was negligible.

To test whether loss of mitochondrial C_{12} FAO capacity is sufficient to recapitulate the macrovesicular steatosis phenotype, we maintained MCADKO and LCADKO mice on the various diets for five weeks. On standard diet, neither knockout strain exhibited visible macrovesicular steatosis upon H& E staining of liver tissue (data not shown). Surprisingly, while MCAD is the predominant ACAD enzyme metabolizing C_8-CoA and C_{10}-CoA, maintaining MCADKO mice on the high-fat C_8/C_{10} diet did not result in increased triglyceride storage (Fig. 7b) or any signs of macrovesicular steatosis following histological staining (data not shown). With the coconut oil diet, both MCADKO and LCADKO mice showed significantly increased liver triglycerides (Fig. 7c), but only LCADKO livers exhibited the periportal macrovesicular steatosis phenotype (Fig. 7d). Immunostaining for

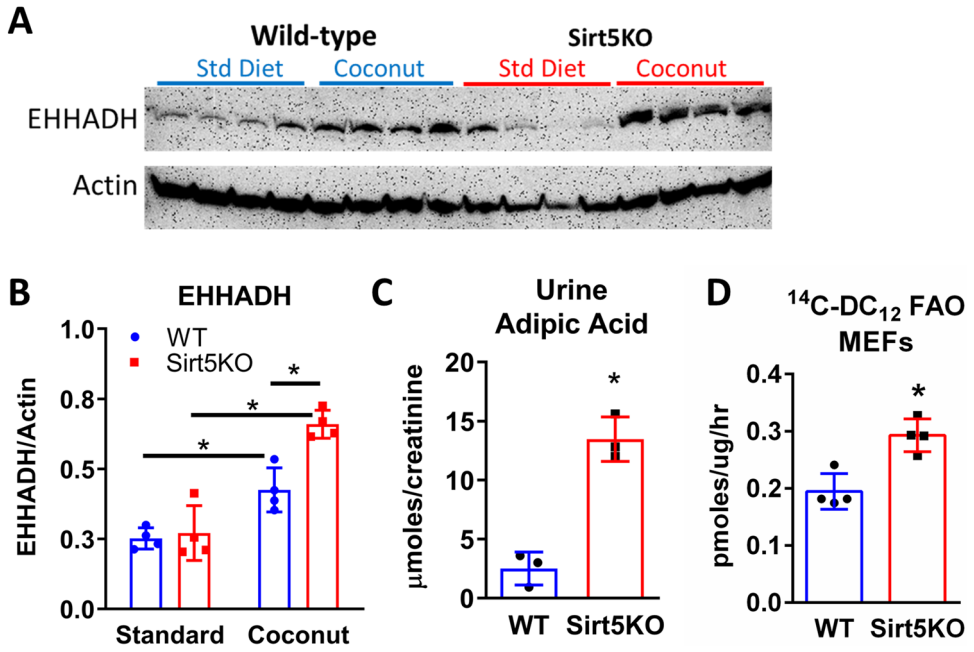

Figure 6. Omega oxidation is upregulated in Sirt5KO livers. **(A)** Immunoblotting for peroxisomal enoyl-CoA hydratase/3-hydroxyacyl-CoA dehydrogenase (EHHADH) in standard diet (SD) and coconut-fed (Coco) wild-type and Sirt5KO livers, N = 4. β-actin served as loading control. The uncropped versions of these blots appear in Supplemental Fig. 4. **(B)** Densitometric analysis of panel **(A)**. *P < 0.01 for indicated pairwise comparisons. **(C)** Urine adipic acid, the peroxisomally-generated product from degradation of the dicarboxylic acids produced by omega oxidation; N = 3 wild-type (WT) and Sirt5KO coconut-fed mice. *P < 0.01. **(D)** Flux of ^{14}C-dicarboxylic (DC) C_{12} to labeled acid-soluble metabolites in cultured mouse embryonic fibroblasts (MEFs), N = 4 replicates. *P < 0.05.

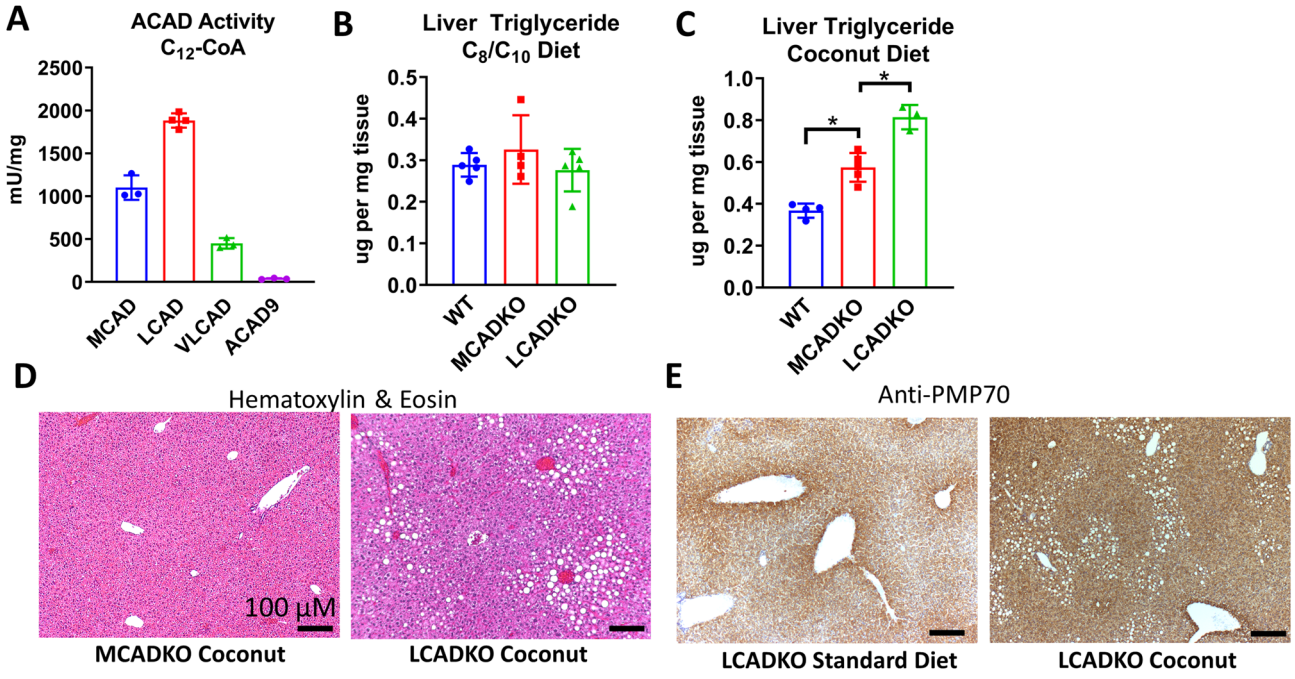

Figure 7. *Loss of mitochondrial FAO causes periportal macrovesicular steatosis on coconut oil diet. (A)* Specific activities of four recombinant mitochondrial acyl-CoA dehydrogenases with C_{12}-CoA as substrate indicates LCAD and MCAD are the predominant C_{12}-utilizing enzymes. **(B,C)** Liver triglyceride content following either five weeks of C_8/C_{10} diet (panel **B**) or coconut oil diet (panel **C**). **(D)** Representative H&E staining of MCADKO and LCADKO liver following five weeks of coconut oil feeding reveals periportal macrovesicular steatosis in LCADKO mice. **(E)** Representative immunostaining for the peroxisomal marker PMP70 in LCADKO mice on either standard diet or coconut-oil diet for five weeks. Scale bar, 100 µM.

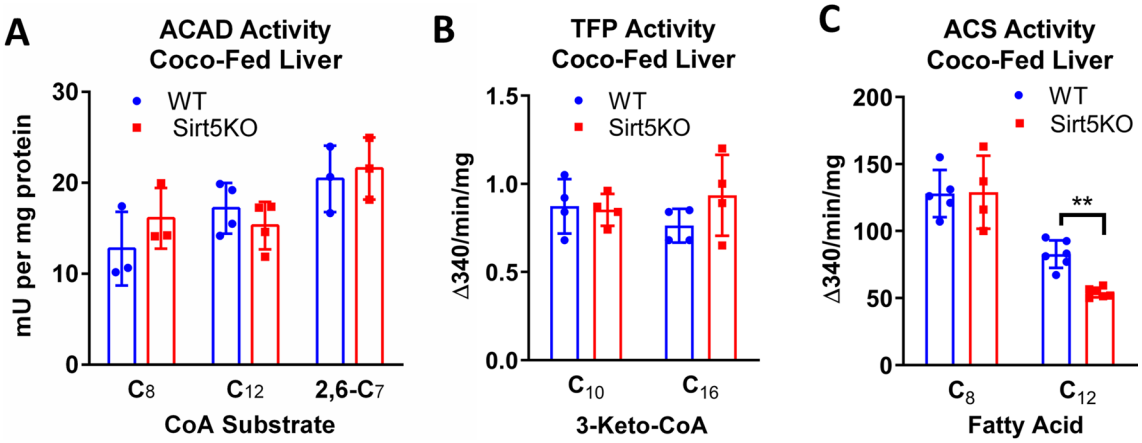

Figure 8. Sirt5KO liver shows reduced activation of C_{12} to C_{12}-CoA. N = 3–5 liver homogenates from coconut-fed wildtype (WT) and Sirt5KO mice were tested for acyl-CoA dehydrogenase (ACAD) enzymatic activity with MCAD and LCAD substrates (panel **A**), mitochondrial trifunctional protein (TFP) activity with medium and long-chain substrates (panel **B**), and mitochondrial acyl-CoA synthetase (ACS) activity with C_8 and C_{12} fatty acids (panel **C**). **P < 0.01.

PMP70 in liver from LCADKO fed coconut oil also revealed a pan-zonal distribution of peroxisomes similar to that observed in Sirt5KO liver (Fig. 7e).

Sirt5KO liver shows reduced activation of C_{12} to C_{12}-CoA. The experiments described above point to a mitochondrial FAO defect in Sirt5KO livers that causes reduced C_{12} oxidation but not C_8 oxidation. C_{12} is the transition point between medium-chain and long-chain fatty acids; it is utilized primarily by the long-chain FAO machinery while C_8 is the optimal chain length for the medium-chain FAO machinery. We therefore hypothesized that reduced function of either LCAD or trifunctional protein (TFP), which together catalyze the four reactions in the long-chain FAO cycle, may explain the C_{12}-specific phenotype. Both LCAD and TFP are heavily acylated enzymes with multiple Sirt5-targeted lysine residues[3], but their activity has not heretofore been measured in Sirt5KO liver. First, the ETF fluorescence reduction assay was used to measure acyl-CoA dehydrogenase activity in liver lysates from coconut-oil fed wild-type and Sirt5KO mice. Three substrates were tested—C_8-CoA, which is specific for MCAD; C_{12}-CoA, which is primarily metabolized by LCAD with overlapping activity from MCAD and very long-chain acyl-CoA dehydrogenase (VLCAD); and 2,6-C_7-CoA, a branched-chain substrate specific for LCAD[29]. There was no statistically significant change in acyl-CoA dehydrogenase activity in Sirt5KO livers with any of the three substrates (Fig. 8a). Next, we measured activity of TFP with both a medium-chain substrate (3-keto-C_{10}-CoA) and a long-chain substrate (3-keto-C_{16}-CoA). As with LCAD, no significant change in TFP activity was observed (Fig. 8b).

Another difference in substrate handling between C_{12} and C_8 is at the acyl-CoA synthetase step, which activates fatty acids to acyl-CoAs prior to FAO. C_8 more readily diffuses through membranes than C_{12} and is activated to C_8-CoA inside the mitochondrial matrix by the ACSMs. C_{12} is a poor substrate for the ACSMs[13]. This suggests that C_{12} is activated by members of the ACSL family. There are no ACSLs in the matrix; rather, they are localized to the outer mitochondrial membrane facing the cytosol as well as on the ER membrane[14]. To determine whether loss of Sirt5 alters activity of the acyl-CoA synthetases, we isolated liver mitochondria and measured conversion rates of ^{14}C–C_8 and ^{14}C–C_{12} to their respective acyl-CoAs. The rate of mitochondrial ^{14}C–C_8 activation was not different between coconut-fed wild-type and Sirt5KO livers while the rate of mitochondrial ^{14}C–C_{12} activation was significantly lower (Fig. 8c).

Discussion

In the nutritional supplement industry, the term MCT is used a catch-all for coconut oil, pure C_8, and mixed C_8/C_{10} products. Our data indicate that these products may be metabolized very differently. C_8/C_{10} feeding resulted in periportal microvesicular steatosis. In mice consuming the C_{12}-rich coconut oil diet this effect was greatly exacerbated, with steatosis spread throughout the liver. Loss of either Sirt5 or the mitochondrial FAO enzyme LCAD pushed the phenotype into macrovesicular steatosis in the periportal zone. Loss of MCAD, a mitochondrial FAO enzyme with high specificity for C_8-CoA/C_{10}-CoA, did not increase triglyceride storage over wildtype levels or cause macrovesicular steatosis on the high C_8/C_{10} diet. Thus, stressing mice partially deficient in mitochondrial C_{12} FAO (Sirt5KO, LCADKO) with a diet rich in C_{12} is a combination sufficient to produce periportal macrovesicular steatosis, while stressing mice deficient in C_8/C_{10} FAO (MCADKO) with a diet rich in C_8/C_{10} does not produce this phenotype. We postulate that this is because C_{12} is metabolized differently than fatty acids that are just 2–4 carbons shorter.

Medium-chain fatty acids are often stated to enter mitochondria by diffusion and rapidly undergo β-oxidation[7]. C_8, the prototypical medium-chain fatty acid, is well known to enter mitochondria independently of the carnitine transport system[30,31]. Etomoxir, an irreversible inhibitor of the key transport enzyme carnitine

palmitoyltransferase-1 (Cpt1), is completely without effect on liver C_8 oxidation[32]. C_{12} has been poorly studied in comparison to C_8. In our experiments, etomoxir blocked C_{12} oxidation by 33% but C_{16} oxidation by 86% (Fig. 5). This indicates that C_{12} partly behaves like a long-chain fatty acid in regard to mitochondrial membrane transport. Perhaps of greater significance is the difference between C_8 and C_{12} in terms of the mechanism of activation to CoA. We observed normal C_8-CoA synthetase activity in Sirt5KO liver but significantly reduced C_{12}-CoA synthetase activity (Fig. 8). This data suggests that the two chain lengths are not activated to CoA by the same enzyme. Liver abundantly expresses two isoforms of medium-chain acyl-CoA synthetase known as ACSM1 and ACSM2. ACSM1 and ACSM2 are localized to the mitochondrial matrix where they activate free medium-chain fatty acids into medium-chain acyl-CoAs for β-oxidation. Vessey et al[13] purified ACSM1 and ACSM2 from human liver mitochondria and characterized reactivity against a range of fatty acid substrates. Interestingly, ACSM1 is 40-fold less active with C_{12} than with C_8, while ACSM2 is 90-fold less active with C_{12}. Thus, if these enzymes are tasked with activating C_{12} that has diffused into the mitochondria, the reaction rate would be predicted to be slow. In contrast, the long-chain acyl-CoA synthetase (ACSL) enzyme family, of which there are four isoforms expressed in liver, exhibit high reactivity with C_{12} and low reactivity with C_8[33,34]. ACSLs are not present in the matrix, but rather are inserted into the outer mitochondrial membrane, ER membrane, and plasma membrane, facing into the cytosol[14]. We previously found multiple Sirt5-targeted lysine residues on ACSL1 and ACSL5[35], but no Sirt5 target sites have been identified on ACSL3 or ACSL4, which are also expressed in liver. Each ACSL activates fatty acids to acyl-CoAs for a different metabolic purpose. For example, ACSL1 is thought to preferentially channel acyl-CoAs into the mitochondria, while ACSL3 has been implicated in lipogenesis[14]. We postulate that decreased activity of ACSL1, but normal activity of ACSL3, could cause partitioning of fatty acids like C_{12} into lipid droplets rather than into mitochondria in Sirt5KO liver.

Another key difference between exogenous C_8 and C_{12} fatty acids is the ability of the latter to be metabolized partially by peroxisomal β-oxidation. Peroxisomes were previously shown to be more abundant in the pericentral zone, which our PMP70 immunostaining confirms[36]. Interestingly, coconut oil feeding appeared to recruit peroxisomes into the periportal zone, such that the anti-PMP70 staining became azonal. PMP70 staining appeared stronger in coconut-fed Sirt5KO liver compared to wild-type (Fig. 5e) yet immunoblotting for the peroxisomal enzyme ACOX1 revealed a trend for lower ACOX1 in Sirt5KO liver (Fig. 5c,d). This apparent discrepancy between peroxisomal abundance (PMP70 staining) and peroxisomal enzyme content (ACOX1) has been reported previously in animals treated with peroxisome-proliferator activated receptor-α (PPARα) agonist drugs and may reflect newly formed peroxisomes that have membrane marker proteins like PMP70 but are largely devoid of peroxisomal matrix proteins[37]. Future work will address whether such a phenomenon may be occurring in Sirt5KO liver with coconut oil feeding. It must also be tested whether C12 can alter the distribution of peroxisomes in human hepatocytes. Peroxisomal biogenesis and the peroxisomal FAO pathway are well known to be more inducible in rodents than in humans, possibly due to the much higher abundance of PPARα in rodent liver[38,39].

While peroxisomes have the capacity to metabolize ^{14}C–C_{12} in liver homogenates when mitochondria are inhibited with KCN, it is not currently possible to determine the relative disposition of C_{12} through peroxisomes versus mitochondria in vivo. What is clear is that increased peroxisome abundance does not prevent lipid accumulation or macrovesicular steatosis in either Sirt5KO or LCADKO livers. Peroxisomes are known to interact directly with lipid droplets[40]. Elimination of some peroxisomal membrane "Pex" proteins results in reduced lipid droplet size, thought to be due to shared biogenesis mechanisms between peroxisomes and lipid droplets[41]. Another interesting possibility requiring future investigation is that periportal peroxisomes in Sirt5KO and LCADKO livers are partially chain-shortening excess C_{12} to acetyl-CoA, which is being released to the cytosol and used for fatty acid synthesis. Intriguingly, the peroxisomal membrane protein PMP70 physically interacts with fatty acid synthase[42]. Further, experiments with ^{13}C-fatty acid tracers showed significant labeling of cytosolic malonyl-CoA, consistent with peroxisomally-produced acetyl-CoA being converted to malonyl-CoA in the cytosol[43,44]. This would not only provide building blocks for fatty acid synthesis, but also further inhibit mitochondrial FAO at the level of Cpt1, leading to a vicious cycle that promotes steatosis.

In summary, this work shows that MCT, and particularly C_{12}-rich coconut oil, is associated with a strongly-zoned pattern of lipid accumulation exacerbated by impaired mitochondrial FAO. People consuming MCT as a dietary supplement are not likely to consume the quantity of MCT that the animals did in our experiments. However, preterm infants, patients with epilepsy and FAO disorders, and other patient groups for whom long-chain fatty acids are contraindicated may consume 40% or more of their calories from MCT. It remains to be seen whether long-term consumption of MCT in these patients leads to NAFLD or other hepatic complications. Finally, it is of note that the periportal macrovesicular steatosis seen in Sirt5KO and LCADKO mice consuming coconut oil resembles pediatric NAFLD[23]. For reasons that are not understood, adult NAFLD begins in the pericentral zones and slowly spreads towards the periportal zones as the disease progresses, while pediatric NAFLD shows the opposite pattern. It is tempting to speculate that impaired FAO may contribute to the development of pediatric NAFLD. The biological roles of both Sirt5 and LCAD in humans are poorly understood. LCAD exhibits a much more restricted expression pattern in human than in rodents[45,46]. LCAD is, however, expressed and active in human liver[47]. Our results here suggest it could play a role in the hepatic response to dietary medium-chain fatty acids. Further, common polymorphisms exist in both the Sirt5 and LCAD genes that may affect expression/activity of these enzymes[48,49]. In any case, the consumption of coconut oil, which is increasingly being incorporated into processed foods, may be contraindicated for children with other known NAFLD risk factors.

Experimental procedures

Animals experimentation. All animal protocols were approved by the University of Pittsburgh Institutional Animal Care and Use Committee (IACUC), and all experiments were conducted in accordance with the guidelines and regulations set forth in the Animal Welfare Act (AWA) and PHS Policy on Humane Care and Use of Laboratory Animals. SIRT5−/− and wildtype control mice were purchased from Jackson Laboratories (Bar Harbor, ME) and bred in-house. LCAD−/− mice and medium-chain acyl-CoA dehydrogenase (MCAD) −/− mice were obtained from the Mutant Mouse Regional Resource Center. All strains are on a mixed background of C57Bl/6 and 129. High-fat diets based on coconut oil (D12331), C_8/C_{10} (D17011004; 60% C_8 and 40% C_{10}), or lard (D12451) were purchased from Research Diets, Inc. Mice were placed onto the high-fat diets for five weeks beginning at age 6–8 weeks. Both genders were used; the gender for a given experiment is specified in "Results". All tissues were collected in non-fasted animals between 9:00 and 11:00 a.m. Euthanasia was conducted using inhaled CO_2 gas according to IACUC recommendations.

Fatty acid oxidation assays. ^{14}C-labeled lauric acid (C_{12}) and palmitic acid (C_{16}) were from PerkinElmer, while ^{14}C-octanoic (C_8) and dodecanedioc (dicarboxylic C_{12}) acids were from Moravek, Inc. All but C_8 were bound to fatty acid-free albumin; C_8 was dissolved in 10 mg/ml α-cyclodextrin. For experiments with Sirt5 knockout mouse embryonic fibroblasts (MEFs), which were a kind gift of Dr. Eric Verdin (Buck Institute), the cells were grown to near confluence in T75 flasks. The cells were harvested and resuspended in DMEM containing 5 mM glucose and 125 µM of labeled fatty acid. Cells were rotated in a 37 °C water bath for 1 h. Then, perchloric acid was added to a final concentration of 0.5 M and $^{14}CO_2$ was evolved, captured, and counted as described[50]. FAO in liver lysates were conducted in similar fashion. Freshly isolated liver was weighed and homogenized in 10 volumes of Mir05 media[51]. The lysate was centrifuged at 500 × *g* for 5 min to remove nuclei and unbroken cells. FAO reactions consisted of 5 µl of lysate in a total reaction volume of 200 µl containing 100 mM sucrose, 10 mM Tris–HCl, 5 mM KH_2PO_4, 0.2 mM EDTA, 0.3% fatty acid-free BSA, 80 mM KCl, 1 mM $MgCl_2$, 0.2 mM L-carnitine, 0.1 mM malate, 0.05 mM coenzyme A, 2 mM ATP, 1 mM DTT, and 125 µM of labeled fatty acid. In some experiments, peroxisomal FAO was measured by inhibiting mitochondria with either 2 mM freshly prepared KCN or by preincubation for 15 min with 100 µM etomoxir. ^{14}C-labeled FAO products were separated from the reactions by extraction with chloroform/methanol and counted.

Immunoblotting. Western blotting was performed after electrophoresis on Criterion SDS polyacrylamide gels (BioRad, Hercules, CA) and transfer to nitrocellulose membranes. Antibodies used were: rabbit anti-succinyllysine (PTM Biolabs), anti-malonyllysine (PTM Biolabs), anti-acyl-CoA oxidase-1 (ACOX1; Abcam), anti-enoyl-CoA hydratase/3-hydroxyacyl-CoA dehydrogenase (EHHADH; Abcam), and anti-β-actin (Proteintech). After incubation with HRP-conjugated secondary antibodies (1:5000) blots were visualized with chemiluminescence. In some experiments the blots were scanned and subjected to densitometric analysis using ImageJ software.

Histology and immunohistochemistry. Fresh portions of liver were fixed in 4% paraformaldehyde and embedded in paraffin, sectioned at 4 µm, and stained with hematoxylin and eosin (H&E) using standard methodology. Another portion of liver was embedded in OCT. frozen, and sectioned at 5–10 µm thick for Oil-Red-O staining. Immunostaining was performed as previously described[50,52] using anti-peroxisomal membrane protein-70 (PMP70; Abcam ab85550 at 1:200) and anti-glutamine synthase (GS; Sigma G2781 at 1:1500). Assessment of histology was performed by the Biospecimen Repository and Processing Core of the Pittsburgh Liver Research Center.

Urine adipic acid. Urine was collected from experimental and control animals over a 24 h period using metabolic caging. Creatinine concentration was determined using a kit (Cayman Chemicals, Inc). Adipate was determined in the context of standard clinical urine organic acid assessment at the Children's Hospital of Pittsburgh Clinical Biochemical Genetics Laboratory[53,54]. Briefly, a volume of urine was utilized equal to 1.0 mM creatinine. A 2-phenylbutyrate internal standard is included. Organic acids were extracted by sequential ethyl ether and acetoacetate extractions. Trimethylsilane derivatization was employed. Analysis utilized Agilent 7890A gas chromatography and 5975C mass spectrometry. All peak areas were normalized to that of 2-phenylbutyrate. Fragmentation patterns of urine analytes were compared to an internally compiled fragmentation library and the fragmentation library of the National Institute for Standards and Technology.

Liver triglyceride content. Approximately 100 mg of liver was weighed, chopped finely and digested in 350 µl of ethanolic KOH at 55 °C overnight. After centrifugation to pellet any undigestible material, the sample volumes were brought to 1.2 ml with 50% EtOH. 200 µl was removed to a new tube and mixed with 215 µl of 1 M $MgCl_2$. Samples were clarified once more by centrifugation at 8000 × g and the supernatant used for assaying glycerol content. Glycerol was assayed spectrophotometrically at 540 nm using a kit (Sigma). Triglyceride content was normalized to tissue weight.

Enzyme activity assays. The anaerobic electron transfer flavoprotein (ETF) fluorescence reduction assay was used to measure acyl-CoA dehydrogenase activities as described[55]. His-tagged recombinant enzymes were purified as described [47]. Assays contained either 150 ng of purified recombinant protein or 200 µg of total liver protein, 2 µM recombinant porcine ETF, and 25 µM acyl-CoA substrate. C_8 and C_{12} acyl-CoAs were from Sigma (St. Louis, MO) and 2,6-dimethylheptanoyl-CoA was from Toronto Research Chemicals, (Toronto, ON). Reduc-

tion of ETF fluorescence was followed for 1 min and used to calculate specific activity normalized to protein concentration. Mitochondrial trifunctional protein (TFP) activity was measured in the reverse direction using 3-ketodecanoyl-CoA (3-keto C_{10}-CoA) and 3-ketopalmitoyl-CoA (3-keto-C_{16}-CoA). Reactions contained 30 µg of liver homogenate and 50 µM substrate in a reaction buffer consisting of 100 mM KPO_4, 50 mM MOPS, 0.1 mM DTT, 0.1% Triton-X100, and 0.15 mM NADH. The conversion of NADH to NAD^+ was followed in a plate reader at 340 nm. C_8 and C_{12}-CoA synthetase activities were measured using ^{14}C-C_8 and ^{14}C-C_{12}. Liver mitochondria were isolated by differential centrifugation and resuspended in cold SET buffer (10 mM Tris–HCl, 250 mM sucrose, 1 mM EDTA). Synthetase reactions (200 µl) contained 5 µl of homogenate with 10 µM ^{14}C-fatty acid in a buffer of 40 mM Tris–HCl, 5 mM ATP, 5 mM $MgCl_2$, 4 mM CoA, 0.8 mg/ml Triton WR1339, and 1 unit/ml inorganic pyrophosphatase. After 2 min incubation at 37 °C, reactions were stopped with sulfuric acid and extracted either four times with ether (C_8-CoA synthetase) or chloroform/methanol (C_{12}-CoA synthetase) to separate formed acyl-CoAs from excess ^{14}C-fatty acid. Activities were normalized to protein concentration.

Received: 2 April 2020; Accepted: 8 October 2020
Published online: 27 October 2020

References

1. Nishida, Y. *et al.* SIRT5 regulates both cytosolic and mitochondrial protein malonylation with glycolysis as a major target. *Mol. Cell* **59**, 321–332. https://doi.org/10.1016/j.molcel.2015.05.022 (2015).
2. Tan, M. *et al.* Lysine glutarylation is a protein posttranslational modification regulated by SIRT5. *Cell Metab.* **19**, 605–617. https://doi.org/10.1016/j.cmet.2014.03.014 (2014).
3. Rardin, M. J. *et al.* SIRT5 regulates the mitochondrial lysine succinylome and metabolic networks. *Cell Metab.* **18**, 920–933. https://doi.org/10.1016/j.cmet.2013.11.013 (2013).
4. Chen, X. F. *et al.* SIRT5 inhibits peroxisomal ACOX1 to prevent oxidative damage and is downregulated in liver cancer. *EMBO Rep.* **19**, https://doi.org/10.15252/embr.201745124 (2018).
5. Zhang, Y. *et al.* SIRT3 and SIRT5 regulate the enzyme activity and cardiolipin binding of very long-chain acyl-CoA dehydrogenase. *PLoS ONE* **10**, e0122297. https://doi.org/10.1371/journal.pone.0122297 (2015).
6. Kapoor, V., Malviya, M. N. & Soll, R. Lipid emulsions for parenterally fed term and late preterm infants. *Cochrane Database Syst. Rev.* **6**, CD013171, https://doi.org/10.1002/14651858.CD013171.pub2 (2019).
7. Gillingham, M. B. *et al.* Triheptanoin versus trioctanoin for long-chain fatty acid oxidation disorders: A double blinded, randomized controlled trial. *J. Inherit. Metab. Dis.* **40**, 831–843. https://doi.org/10.1007/s10545-017-0085-8 (2017).
8. Borges, K., Kaul, N., Germaine, J., Kwan, P. & O'Brien, T. J. Randomized trial of add-on triheptanoin vs medium chain triglycerides in adults with refractory epilepsy. *Epilepsia Open* **4**, 153–163. https://doi.org/10.1002/epi4.12308 (2019).
9. Shah, N. D. & Limketkai, B. N. The use of medium-chain triglycerides in gastrointestinal disorders. *Pract. Gastroenterol.* **160**, 20–28 (2017).
10. Sankararaman, S. & Sferra, T. J. Are we going nuts on coconut oil?. *Curr. Nutr. Rep.* **7**, 107–115. https://doi.org/10.1007/s13668-018-0230-5 (2018).
11. St-Pierre, V. *et al.* Plasma ketone and medium chain fatty acid response in humans consuming different medium chain triglycerides during a metabolic study day. *Front. Nutr.* **6**, 46. https://doi.org/10.3389/fnut.2019.00046 (2019).
12. Boateng, L., Ansong, R., Owusu, W. B. & Steiner-Asiedu, M. Coconut oil and palm oil's role in nutrition, health and national development: A review. *Ghana Med. J.* **50**, 189–196 (2016).
13. Vessey, D. A., Kelley, M. & Warren, R. S. Characterization of the CoA ligases of human liver mitochondria catalyzing the activation of short- and medium-chain fatty acids and xenobiotic carboxylic acids. *Biochim. Biophys. Acta* **1428**, 455–462. https://doi.org/10.1016/s0304-4165(99)00088-4 (1999).
14. Grevengoed, T. J., Klett, E. L. & Coleman, R. A. Acyl-CoA metabolism and partitioning. *Annu. Rev. Nutr.* **34**, 1–30. https://doi.org/10.1146/annurev-nutr-071813-105541 (2014).
15. Piot, C., Hocquette, J. F., Veerkamp, J. H., Durand, D. & Bauchart, D. Effects of dietary coconut oil on fatty acid oxidation capacity of the liver, the heart and skeletal muscles in the preruminant calf. *Br. J. Nutr.* **82**, 299–308 (1999).
16. Christensen, E., Gronn, M., Hagve, T. A. & Christophersen, B. O. Omega-oxidation of fatty acids studied in isolated liver cells. *Biochim. Biophys. Acta* **1081**, 167–173 (1991).
17. Ferdinandusse, S. *et al.* Clinical, biochemical, and mutational spectrum of peroxisomal acyl-coenzyme A oxidase deficiency. *Hum. Mutat.* **28**, 904–912. https://doi.org/10.1002/humu.20535 (2007).
18. 18Tserng, K. Y. & Jin, S. J. Metabolic conversion of dicarboxylic acids to succinate in rat liver homogenates. A stable isotope tracer study. *J. Biol. Chem.* **266**, 2924–2929 (1991).
19. Watkins, P. A., Maiguel, D., Jia, Z. & Pevsner, J. Evidence for 26 distinct acyl-coenzyme A synthetase genes in the human genome. *J. Lipid Res.* **48**, 2736–2750. https://doi.org/10.1194/jlr.M700378-JLR200 (2007).
20. Tucci, S., Primassin, S., Ter Veld, F. & Spiekerkoetter, U. Medium-chain triglycerides impair lipid metabolism and induce hepatic steatosis in very long-chain acyl-CoA dehydrogenase (VLCAD)-deficient mice. *Mol. Genet. Metab.* **101**, 40–47. https://doi.org/10.1016/j.ymgme.2010.05.005 (2010).
21. Narayanankutty, A., Palliyil, D. M., Kuruvilla, K. & Raghavamenon, A. C. Virgin coconut oil reverses hepatic steatosis by restoring redox homeostasis and lipid metabolism in male Wistar rats. *J. Sci. Food Agric.* **98**, 1757–1764. https://doi.org/10.1002/jsfa.8650 (2018).
22. Panchal, S. K., Carnahan, S. & Brown, L. Coconut products improve signs of diet-induced metabolic syndrome in rats. *Plant Foods Hum. Nutr.* **72**, 418–424. https://doi.org/10.1007/s11130-017-0643-0 (2017).
23. Africa, J. A. *et al.* In children with nonalcoholic fatty liver disease, zone 1 steatosis is associated with advanced fibrosis. *Clin. Gastroenterol. Hepatol.* **16**, 438–446 e431, https://doi.org/10.1016/j.cgh.2017.02.030 (2018).
24. Li, L. *et al.* PGC-1alpha promotes ureagenesis in mouse periportal hepatocytes through SIRT3 and SIRT5 in response to glucagon. *Sci. Rep.* **6**, 24156. https://doi.org/10.1038/srep24156 (2016).
25. Oaxaca-Castillo, D. *et al.* Biochemical characterization of two functional human liver acyl-CoA oxidase isoforms 1a and 1b encoded by a single gene. *Biochem. Biophys. Res. Commun.* **360**, 314–319. https://doi.org/10.1016/j.bbrc.2007.06.059 (2007).
26. Mortensen, P. B. & Gregersen, N. The biological origin of ketotic dicarboxylic aciduria. In vivo and in vitro investigations of the omega-oxidation of C6–C16-monocarboxylic acids in unstarved, starved and diabetic rats. *Biochim. Biophys. Acta* **666**, 394–404, https://doi.org/10.1016/0005-2760(81)90298-8 (1981).
27. Ding, J. *et al.* The peroxisomal enzyme L-PBE is required to prevent the dietary toxicity of medium-chain fatty acids. *Cell Rep.* **5**, 248–258. https://doi.org/10.1016/j.celrep.2013.08.032 (2013).

28. Wanders, R. J., Ruiter, J. P., L, I. J., Waterham, H. R. & Houten, S. M. The enzymology of mitochondrial fatty acid beta-oxidation and its application to follow-up analysis of positive neonatal screening results. *J. Inherit. Metab. Dis.* **33**, 479–494, https://doi.org/10.1007/s10545-010-9104-8 (2010).
29. Wanders, R. J., Denis, S., Ruiter, J. P., L, I. J. & Dacremont, G. 2,6-Dimethylheptanoyl-CoA is a specific substrate for long-chain acyl-CoA dehydrogenase (LCAD): Evidence for a major role of LCAD in branched-chain fatty acid oxidation. *Biochim. Biophys. Acta* **1393**, 35–40, https://doi.org/10.1016/s0005-2760(98)00053-8 (1998).
30. Nakajima, T. *et al.* The effect of carnitine on ketogenesis in perfused livers from juvenile visceral steatosis mice with systemic carnitine deficiency. *Pediatr. Res.* **42**, 108–113. https://doi.org/10.1203/00006450-199707000-00017 (1997).
31. Bremer, J. Carnitine—Metabolism and functions. *Physiol. Rev.* **63**, 1420–1480. https://doi.org/10.1152/physrev.1983.63.4.1420 (1983).
32. Sidossis, L. S., Stuart, C. A., Shulman, G. I., Lopaschuk, G. D. & Wolfe, R. R. Glucose plus insulin regulate fat oxidation by controlling the rate of fatty acid entry into the mitochondria. *J. Clin. Investig.* **98**, 2244–2250. https://doi.org/10.1172/JCI119034 (1996).
33. Iijima, H. *et al.* Biochemical studies of two rat acyl-CoA synthetases, ACS1 and ACS2. *Eur. J. Biochem.* **242**, 186–190. https://doi.org/10.1111/j.1432-1033.1996.0186r.x (1996).
34. Fujino, T., Kang, M. J., Suzuki, H., Iijima, H. & Yamamoto, T. Molecular characterization and expression of rat acyl-CoA synthetase 3. *J. Biol. Chem.* **271**, 16748–16752. https://doi.org/10.1074/jbc.271.28.16748 (1996).
35. Zhang, Y. *et al.* Lysine desuccinylase SIRT5 binds to cardiolipin and regulates the electron transport chain. *J. Biol. Chem.* **292**, 10239–10249. https://doi.org/10.1074/jbc.M117.785022 (2017).
36. Guzman, M., Bijleveld, C. & Geelen, M. J. Flexibility of zonation of fatty acid oxidation in rat liver. *Biochem. J.* **311**(Pt 3), 853–860. https://doi.org/10.1042/bj3110853 (1995).
37. Fahimi, H. D. & Baumgart, E. Current cytochemical techniques for the investigation of peroxisomes. A review. *J. Histochem. Cytochem.* **47**, 1219–1232. https://doi.org/10.1177/002215549904701001 (1999).
38. Kersten, S. Integrated physiology and systems biology of PPARalpha. *Mol. Metab.* **3**, 354–371. https://doi.org/10.1016/j.molmet.2014.02.002 (2014).
39. Vamecq, J., Cherkaoui-Malki, M., Andreoletti, P. & Latruffe, N. The human peroxisome in health and disease: The story of an oddity becoming a vital organelle. *Biochimie* **98**, 4–15. https://doi.org/10.1016/j.biochi.2013.09.019 (2014).
40. Schrader, M., Kamoshita, M. & Islinger, M. Organelle interplay-peroxisome interactions in health and disease. *J. Inherit. Metab. Dis.* **43**, 71–89. https://doi.org/10.1002/jimd.12083 (2020).
41. Joshi, A. S. *et al.* Lipid droplet and peroxisome biogenesis occur at the same ER subdomains. *Nat. Commun.* **9**, 2940. https://doi.org/10.1038/s41467-018-05277-3 (2018).
42. Hillebrand, M. *et al.* Identification of a new fatty acid synthesis-transport machinery at the peroxisomal membrane. *J. Biol. Chem.* **287**, 210–221. https://doi.org/10.1074/jbc.M111.272732 (2012).
43. Kasumov, T. *et al.* Probing peroxisomal beta-oxidation and the labelling of acetyl-CoA proxies with [1-(13C)]octanoate and [3-(13C)]octanoate in the perfused rat liver. *Biochem. J.* **389**, 397–401. https://doi.org/10.1042/BJ20050144 (2005).
44. Reszko, A. E. *et al.* Peroxisomal fatty acid oxidation is a substantial source of the acetyl moiety of malonyl-CoA in rat heart. *J. Biol. Chem.* **279**, 19574–19579. https://doi.org/10.1074/jbc.M400162200 (2004).
45. Maher, A. C., Mohsen, A. W., Vockley, J. & Tarnopolsky, M. A. Low expression of long-chain acyl-CoA dehydrogenase in human skeletal muscle. *Mol. Genet. Metab.* **100**, 163–167. https://doi.org/10.1016/j.ymgme.2010.03.011 (2010).
46. Chegary, M. *et al.* Mitochondrial long chain fatty acid beta-oxidation in man and mouse. *Biochim. Biophys. Acta* **1791**, 806–815. https://doi.org/10.1016/j.bbalip.2009.05.006 (2009).
47. Zhang, Y., Bharathi, S. S., Beck, M. E. & Goetzman, E. S. The fatty acid oxidation enzyme long-chain acyl-CoA dehydrogenase can be a source of mitochondrial hydrogen peroxide. *Redox Biol.* **26**, 101253. https://doi.org/10.1016/j.redox.2019.101253 (2019).
48. Beck, M. E. *et al.* The common K333Q polymorphism in long-chain acyl-CoA dehydrogenase (LCAD) reduces enzyme stability and function. *Mol. Genet. Metab.* https://doi.org/10.1016/j.ymgme.2020.04.005 (2020).
49. Glorioso, C., Oh, S., Douillard, G. G. & Sibille, E. Brain molecular aging, promotion of neurological disease and modulation by sirtuin 5 longevity gene polymorphism. *Neurobiol. Dis.* **41**, 279–290. https://doi.org/10.1016/j.nbd.2010.09.016 (2011).
50. Chiba, T. *et al.* Sirtuin 5 regulates proximal tubule fatty acid oxidation to protect against AKI. *J. Am. Soc. Nephrol.* **30**, 2384–2398. https://doi.org/10.1681/ASN.2019020163 (2019).
51. Komlodi, T. *et al.* Comparison of mitochondrial incubation media for measurement of respiration and hydrogen peroxide production. *Methods Mol. Biol.* **1782**, 137–155. https://doi.org/10.1007/978-1-4939-7831-1_8 (2018).
52. Russell, J. O. *et al.* Hepatocyte-specific beta-catenin deletion during severe liver injury provokes cholangiocytes to differentiate into hepatocytes. *Hepatology* **69**, 742–759. https://doi.org/10.1002/hep.30270 (2019).
53. Thompson, J. A. & Markey, S. P. Quantitative metabolic profiling of urinary organic acids by gas chromatography-mass spectrometry: Comparison of isolation methods. *Anal. Chem.* **47**, 1313–1321. https://doi.org/10.1021/ac60358a074 (1975).
54. Gates, S. C., Dendramis, N. & Sweeley, C. C. Automated metabolic profiling of organic acids in human urine. I. Description of methods. *Clin. Chem.* **24**, 1674–1679 (1978).
55. Bharathi, S. S. *et al.* Sirtuin 3 (SIRT3) protein regulates long-chain acyl-CoA dehydrogenase by deacetylating conserved lysines near the active site. *J. Biol. Chem.* **288**, 33837–33847. https://doi.org/10.1074/jbc.M113.510354 (2013).

Author contributions

E.S.G. designed experiments, coordinated the study, performed experiments, analyzed data, and wrote the manuscript. S.S.B., Y.Z., X-J.Z., and K.P. performed experiments, assisted with data analysis, and contributed to the Methods section. S.F.D. was responsible for the urine adipic acid mass spectrometry and interpretation, and contributed to the Methods section. S.S-L. edited the manuscript. S.P.M. interpreted histopathological slides and immunohistochemistry stains and edited the manuscript. All authors discussed the final data and commented on the manuscript.

Funding

This study was funded by NIH grant DK090242 (ESG) and in part by 1R01DK62277 (SPM), and 1R01DK100287 (SPM) and P30DK120531 (Pittsburgh Liver Research Center).

Competing interests

The authors declare no competing interests.

Additional information

Supplementary information is available for this paper at https://doi.org/10.1038/s41598-020-75615-3.

Correspondence and requests for materials should be addressed to E.S.G.